

# LARGE EDDY SIMULATION OF AN UNSTEADY LIFTED FLAME

**Christophe Duwig**

Div. of Fluid Mechanics, Dept. Energy Sciences  
Lund University – Box 118  
SE- 22100 Lund, Sweden  
Christophe.Duwig@vok.lth.se

**Laszlo Fuchs**

Div. of Fluid Mechanics, Dept. Energy Sciences  
Lund University – Box 118  
SE- 22100 Lund, Sweden  
Laszlo.Fuchs@vok.lth.se

## ABSTRACT

A lifted turbulent flame in a vitiated co-flow is studied using Large Eddy Simulation together with a perfectly stirred reactor based closure. The closure generates chemical look-up tables that are further used to close the filtered temperature equations and to compute local radical concentrations throughout the computational domain. The two-scalar approach has been used to simulate a lifted turbulent flame. The numerical predictions are compared to detailed experimental data obtained by Cabra et al. (2002). The agreement between the two sets of data is very good indicating that the present approach predicts successfully the flame lift-off and the combustion process.

The LES data is also used to study the unsteady flame stabilization. The influence of the large scale turbulent structures on the fuel/air mixing as well as on the combustion is highlighted.

## INTRODUCTION

Turbulent combustion is a difficult topic involving non-linear multi-scale phenomena. As a result, turbulent flames are complex and often difficult to stabilize in practice. In order to have a flame, one needs at the given location there is enough fuel and oxidant and high enough temperature. If one of the components is missing, the oxidation can not proceed and there is a risk of flame blow-out. At high Reynolds numbers, the co-existence of these three factors depends highly on the turbulent mixing. Consequently, the flame location is unsteady in nature and very sensitive to perturbations; (c.f. Poinso and Veynante, 2001). Such an example is given by Cabra et al. (2002) for a non-premixed lifted jet flame where the flame starts at some 10 diameters downstream of the nozzle. The high sensitivity of the flame stresses the importance and the need for a better understanding of the flame dynamics and stabilization.

In the present paper we investigate a non-premixed lifted flame corresponding to the vitiated co-flow burner (VCB) experiment conducted by Cabra et al. (2002). The flame is well documented. The data has been acquired by non-intrusive laser measurements techniques. However, the unsteady features of the stabilization have not been

explored so far. Since we focus on unsteady features of the turbulent flame, we use reacting Large Eddy Simulation (LES) to study the lift-off and stabilization of the VCB flame. Firstly, we present the LES governing equations. Secondly, the combustion model together with the chemistry tabulation technique is listed. Thirdly, we present the computational case and boundary conditions. In the result section, the numerical predictions are compared with the experimental data and used to study the stabilization of the flame.

## GOVERNING EQUATIONS FOR TURBULENT FLOWS

### Momentum equations and closure

The basic equations describing the motion of a fluid are the conservation of momentum, mass, species and energy (Poinso and Veynante, 2001). The system of equations has to be closed with an equation of state. In LES, one applies a low-pass filter to the dependent variables so that the filtered governing equations only describe the larger turbulent fluctuations. They read:

$$\frac{\partial \bar{\rho}}{\partial t} + \nabla \cdot \bar{\rho} \mathbf{u} = 0 \quad (1)$$

$$\frac{\partial \bar{\rho} \mathbf{u}}{\partial t} + \nabla \cdot (\bar{\rho} \tilde{\mathbf{u}} \tilde{\mathbf{u}}) = -\nabla \bar{p} + \nabla \cdot (\bar{\rho} \tilde{\mathbf{u}} \tilde{\mathbf{u}} - \overline{\rho \mathbf{u} \mathbf{u}} + \overline{\mu \nabla \mathbf{u}}) \quad (2)$$

The filtering operator is linear and is assumed to be commutative with time- and space-derivatives. The filtering operation is not commutative with non-linear terms. Thus, the non-linear terms lead to expressions that cannot be expressed in terms of the filtered quantities. These terms are gathered on the right-hand side in the equations above and are called collectively as the subgrid scale (SGS) term. We model the SGS term by a classical gradient expression with an effective 'eddy' viscosity  $\mu_\Delta$  based on the Filtered Structure Function Model (Ducros et al., 1996) so that:

$$\mu_\Delta = \bar{\rho} C_\Delta \sqrt{(F_2(HP(\tilde{\mathbf{u}})))} \quad (3)$$

where  $F_2$  denotes the structure function computed from the filtered resolved flow field,  $C$  is a constant and  $HP$  is a high-pass filter.

### Combustion closure

Incorporating combustion chemistry into LES involves finding a suitable reaction mechanism and solving a reduced set of filtered species equations. In non-premixed flames, one conveniently introduces the mixture fraction  $Z$  (Poinso and Veynante, 2001) to describe the fuel air mixing ( $Z=1$  in the fuel and  $Z=0$  in the oxidant). Considering a fuel fluid parcel that enters, a typical scenario is as follow:

- The fuel fluid parcel is convected and travels down stream.
- The fuel fluid parcel mixes with the hot oxidant.  $Z$  increases during the mixing process. No reactions occur at this stage. The fluid parcel composition changes as fuel and oxygen are diluted and the local temperature increases.
- The fluid parcel composition and temperature are such that auto-ignition occurs.
- The combustion proceeds in the parcel. The flame may interact with neighboring parcels.
- The parcel leaves the combustor.

One represents the scenario as an unsteady Perfectly Stirred Reactor (PSR) (Duwig et al., 2006). The set of equations describing the idealized process are:

$$\begin{cases} \rho \frac{dY_i}{dt} = \dot{w}_i, \quad i = 1, \dots, N, \\ \rho \frac{dT}{dt} = \dot{w}_T \end{cases} \quad (4)$$

The initial conditions for the  $N$  species and temperature are:

$$X(t=0) = \begin{bmatrix} Y_i \\ T \end{bmatrix} = Z \cdot X_{FUEL} + (1-Z) \cdot X_{OXIDANT} \quad (5)$$

where the subscripts  $FUEL$  and  $OXIDANT$  denote the cold fuel and vitiated air respectively. Equations (4) are ODE (Ordinary Differential Equations) and are easily solved using chemical packages together with detailed reaction mechanisms. In the present work, a comprehensive  $H_2/O_2$  mechanism is used (Li et al., 2004) together with the software CANTERA (2005). The solution of the ODE is mapped in a  $[Z, T]$  coordinate system providing a complete description of the chemical state (species mole fractions and reaction rates) as function of two scalars only.

As a consequence, only two scalar transport equations are needed. Firstly, the mixture fraction transport equation reads:

$$\bar{\rho} \partial_t \tilde{Z} + \overline{\rho u} \cdot \nabla \tilde{Z} = \nabla \cdot ((\rho D + \rho D_\Delta \nabla \tilde{Z})). \quad (6)$$

Secondly, the corresponding filtered temperature equation is:

$$\bar{\rho} \partial_t \tilde{T} + \overline{\rho u} \cdot \nabla \tilde{T} = \nabla \cdot (\rho D_T + \rho D_\Delta \nabla \tilde{T}) + \overline{\dot{w}_T(Z, T)} \quad (7)$$

Among the different closures options (Poinso and Veynante, 2001), we use a presumed filtered density function (FDF) approach so that the closure reads:

$$\overline{\dot{w}_T(Z, T)} = \iint \dot{w}_T(Z, T) \cdot P(\tilde{Z}, \tilde{T}, Z, T, \dots) dZdT \quad (8)$$

where  $P$  is the FDF taken to be a top-hat function and the local SGS variance is computed analytically (Pierce and Moin, 1998). The reaction rate  $\dot{w}_T(Z, T)$  is obtained from the tabulation of the solution of Equation (4).

## COMPUTATIONAL TOOL AND CASE

### LES code

We use a high-order finite difference code that solves a low-Mach number formulation of the Navier-Stokes equations on Cartesian grids (Gullbrand et al., 2001). The spatial discretization is done using a fourth order centered scheme except for the convective terms in equations (5-6) that are treated using 5<sup>th</sup> order Weighted Essentially Non Oscillatory scheme (Jiang and Shu, 1996) ensuring stability and high order accuracy. A second order finite difference scheme is used for time discretization, the time integration is done implicitly. Locally refined grids are employed in regions with large gradients. Multi-grid iterations are used to solve the implicit parts of the system. More details can be found in Gullbrand et al. (2001). Using Cartesian finite differences techniques provides fast and accurate results. These advantages make the present approach suitable for LES of turbulent flows.

### Geometry and computational grid

The combustor consists of a high speed fuel jet (of diameter  $d=0.00457$ m) surrounded by a low velocity vitiated co-flow i.e. a hot oxidant (Cabra et al., 2002). The diameter of the co-flow is 0.21m so that interaction with the surrounding air can be neglected (Cabra et al., 2002). The operating conditions as well as the molar fractions of the fuel and oxidizer are summarized in Table 1.

The computational domain is a  $22d \cdot 11d \cdot 11d$  box starting at the exit of the fuel nozzle. The coordinate system consists of 3 directions (x, y, z) with x being the streamwise direction. The origin of the coordinate system is taken at the center of the fuel nozzle. Since the mean flow field is axi-symmetric, it is convenient to replace the y- and z- directions by the radius r. The computational grid contains  $\sim 2 \cdot 10^6$  mesh-points with  $\sim 20$  cells across the fuel nozzle. The resolution is adequate for studying the large scales in this type of problem.

The time step is set by ensuring the Courant number does not exceed 0.3. Following results are normalized by the fuel jet bulk velocity  $U_0=107$  m/s and the fuel pipe diameter  $d$  with a corresponding time unit  $\tau=d/U_0=4.3 \cdot 10^{-5}$  s. The averaging was performed over a time span of approximately  $1000 \tau$ .

The vortex core has been visualized using a criteria based on the second largest eigenvalue of the second invariant of the velocity derivative tensor proposed by Jeong and Hussain (1995) (the so-called  $\lambda_2$  technique). In the following figures the vortex core corresponds to a region where the eigenvalue  $\lambda_2$  is negative.

Table 1: Boundary conditions for the H<sub>2</sub>/N<sub>2</sub> flame including species molar fractions (Cabra et al., 2002).

|         | U<br>[m/s] | T<br>[K] | H <sub>2</sub> | H <sub>2</sub> O | N <sub>2</sub> | O <sub>2</sub> |
|---------|------------|----------|----------------|------------------|----------------|----------------|
| Fuel    | 107.0      | 305      | 0.25           | 0.00             | 0.75           | 0.00           |
| Oxidant | 3.5        | 1045     | 0.00           | 0.10             | 0.75           | 0.15           |

### Boundary conditions

The boundary conditions are essential for all computational results and in particular for LES. One may approximate the flow using a well defined (mean) velocity profile and adding artificially generated turbulent fluctuations. We consider the decomposition using the time averaging operator  $\langle \cdot \rangle$ :

$$\tilde{u}(x, t) = \langle u \rangle(x) + u'(x) \cdot F(t) \quad (9)$$

Here we set  $\langle u \rangle(x)$  and  $u'(x)$  in order to recover the mean velocity and fluctuation profile of a fully developed pipe flow. It requires the function  $F(t)$  providing a seemingly turbulent fluctuation. We used a digital filter based technique summarized in (Klein et al., 2003).

At the outlet, all variables are assumed to have a zero gradient.

### RESULTS

Figure 1 shows the mean and instantaneous temperature field as predicted by the LES computation. The mean flow field is axi-symmetric and exhibit smooth gradients only. The flame consists of a cold jet surrounded by hot gases. High temperatures (i.e. above the co-flow temperature) are seen relatively far downstream of the fuel nozzle exit indicating that the flame is lifted. Following Cabra et al. (2002), the lift-off height  $x_{IG}$  is defined as  $\langle T(r/d=1.53, x_{IG}) \rangle = 1200\text{K}$  where the operator  $\langle \cdot \rangle$  indicates time averaging. Figure 1 also presents a snapshot of the temperature field. The flame is irregular with steep gradients. Close to the fuel nozzle, the jet is weakly wrinkled. Further downstream, the jet pattern change exhibiting larger wrinkling. Downstream of the lift-off height, the shape of the jet is somehow spirally indicating that turbulent structures as of the order of the jet diameter. Figure 2 shows a snapshot of the mixture fraction. The jet core (i.e. pure fuel) extends approximately  $7d$  downstream of the fuel nozzle. At locations  $(x-x_{IG})/d \sim 0$ , the jet core breaks down and fuel and air are mixing. As pointed out previously this location is characterized by relatively large turbulent structures explaining the jet core breakdown. Although the mixing is relatively intense, we notice that the fuel concentration remains higher along the axis. It follows that the burnt gas temperature is also higher in the region close to the centre-line as shown on Figure 1.

Figure 2 also presents a snapshot of the OH mole-fraction field. The OH mole-fractions are not significant upstream of  $(x-x_{IG})/d \sim 0$  with a sudden raise at this location. We note that the flame is not attached on the stoichiometric line. Close to the fuel nozzle, the stretch in the jet shear-layer (where the stoichiometric level lies) is strong preventing the flame to establish. Instead, fuel and

vitiated air mix. In addition, the flame does lie somehow on the lean side of the stoichiometric line (SL). Actually, the flame is not centred on the SL (as one would expect for a diffusion-type of flame). In the present case, SL indicates rather the rich limit of the OH field. As pointed out, the lift-off enables the fuel and air to mix resulting in a stratified premixed combustion system rather than in a diffusion-type flame.

Figures 3 show the mean temperature field as well as the Root-Mean-Squared (RMS) of the temperature fluctuation. Regarding the mean temperature field, the agreement between the LES and experimental data (Cabra and Dibble, 2002) is good. The discrepancies between the two sets are below the experimental uncertainty except close to the axis at  $(x-x_{IG})/d \sim 3$ . The LES captures well the fuel/air mixing upstream of the flame as well as the flame development along the line  $r/d \sim 1.5$ . The LES also captures well the temperature fluctuations both upstream from the flame (mixing driven fluctuations) and downstream from the flame (combustion and mixing driven fluctuations). The experimental and LES data sets indicate a peak of fluctuation at  $r/d \sim 1$ . The positions and magnitudes of the peaks are well captured but some discrepancies are seen. However, since no uncertainty estimate was provided regarding the RMS fields, it is unclear if these discrepancies are significant. Note that the temperature fluctuation levels are up to 300K (i.e. 30% of the mean temperature). These large levels can be explained by intermittency. For instance, Figures 1 and 2 show that the tip of the jet corresponds to pockets of cold fuel. At a given point in the region  $(x-x_{IG})/d \sim 3$ ,  $r/d \sim 1$ , pockets of cold fuel will alternate with pockets of hot burnt gases inducing strong temperature fluctuations.

Figure 4 shows a snapshot of the temperature and  $\lambda_2$  iso-surfaces. The iso-level  $T=400\text{K}$  corresponds to the jet core while the level  $T=1046\text{K}$  delimits the region of burning/ burnt gases. The figure depicts large scale cortices. Rings line vortices are formed in the jet shear-layer. These rings might merge to give spiral like structures. Further downstream, these are relatively well organized structures but they breakdown into smaller much less organized vortex tubes further downstream. This evolution of the vortices affects the shape of the fuel jet as pointed out previously. At the location of the flame, the vortex tubes are un-organized and no clear turbulent macro-structure is seen. Figure 5 presents an enlargement of the stabilization region. The tip of the fuel jet core is seen to be irregular with a strongly wrinkled surface. Pockets of fuel detach from the tip and are convected downstream as discussed above. The flame region consists of an annulus of relatively high temperature surrounding the tip of the jet core. The shape of the flame is irregular.

Figure 6 presents the time evolution of the temperature and velocity fields along a line  $r/d=1$ . Velocity fluctuations correspond to vortices that are shed in the jet shear-layer. At the present radial location, the vortices trace is seen from  $(x-x_{IG})/d \sim -5$ . These vortices are convected downstream by the mean flow with a speed of  $c \sim 0.5 \cdot U_0$ . Similar pattern are seen on the temperature plot. Upstream of the flame location, some white stripes are seen. They correspond to the entrainment of cold fuel by the vortices shown on Figure 4. Further downstream, dark

regions (i.e. of high temperature) are seen indicating that combustion has started. In the region  $0 < (x-x_{IG})/d < 5$ , alternating black and white stripes are seen resulting in large RMS fields (as seen on Figure 3). The black and white stripes correspond to the fluctuations in axial velocity highlighting the influence of the vortices on the flame dynamics. In addition, the temperature fluctuations have the same convection speed  $c \sim 0.5 \cdot U_0$ . Finally, a statistical analysis (not presented here) at  $(x-x_{IG})/d \sim 3$  of the occurrence of stripes did not show any particular periodic pattern. It is not surprising since the vortex tubes are distributed irregularly as shown on Figure 4.

## SUMMARY

Large Eddy Simulation of a lifted turbulent flame has been performed using a two-scalar approach accounting for complex chemistry effects. The results were shown to be well in line with the experimental data with discrepancies below the experimental uncertainty. Further, the LES data were analyzed in order to highlight the effect of large scale turbulent structures on the flame stabilization. The stabilization mechanism was identified. It consists of:

1. The round fuel jet issues in the vitiated co-flow. Ordered turbulent structures (rings, spirals) stir the fuel and vitiated air. No reaction occurs so far.
2. The turbulent macro-structures breakdown into small scale irregularly distributed structures. It results a small scale mixing.
3. The resulting combustible mixture ignites on the lean side of the shear-layer.
4. Turbulent structures are responsible for stirring of fresh fuel and burnt gases. These structures are convected at a speed of  $c \sim 0.5 \cdot U_0$  and induce an intense intermittency in the temperature field.

## ACKNOWLEDGMENTS

This work has been supported partially by the Swedish Energy Agency (STEM) and partially by the Swedish Research Council (VR). The computations have been performed at LUNARC (Centre for Scientific and Technical Computing at Lund University) and HPC2N (High Performance Computing Centre North) facilities within the SNAC/SNIC allocation program.

The authors want to thank Dr. Markus Klein (TU-Darmstadt, Germany) for kindly providing the code for generating the unsteady inflow conditions.

## REFERENCES

- Cabra R., Dibble R.W., 2002, "Berkeley Jet Flames in a Vitiated Coflow", <http://www.me.berkeley.edu/cal/VCB/Data/>
- Cabra R., Myrhhvold T., Chen J-Y., Dibble R.W., Karpetis A.N., Barlow R.S., 2002, "Simultaneous laser Raman-Rayleigh-LIF measurements and numerical modeling results of a lifted H<sub>2</sub>/N<sub>2</sub> jet flame in a vitiated coflow", *Proc. Comb. Inst.*, Vol. 29, pp. 1881-1888.
- CANTERA, 2005, Object-Oriented Software for Reacting Flows, <http://www.cantera.org>
- Ducros F., Comte P., Lesieur M., 1996, "Large-eddy Simulation of Transition to Turbulence in a Boundary Layer Spatially Developing over a Flat Plate", *J. Fluid Mech.*, Vol. 326, pp. 1-36.
- Duwig C., Szasz R., Fuchs L., 2006, "Modeling of flameless combustion using large eddy simulation", in *Proc. TurboExpo 2006*, ASME Paper GT-2006-90063
- Gullbrand J., Bai X.S., Fuchs L., 2001, "High-order Cartesian Grid Method for Calculation of Incompressible Turbulent Flows", *Int. J. Num. Meth. Fluids*, Vol. 36, pp. 687-709.
- Jeong J., Hussain F., 1995, "On the Identification of a Vortex", *J. Fluid Mech.*, Vol. 285, pp. 69-94.
- Jiang G.S., Shu C.W., 1996, "Efficient Implementation of Weighted ENO Schemes", *J. Comp. Phys.* Vol. 126, p 202.
- Klein M., Sadiki A., Janicka J., 2003, "A digital filter based generation of inflow data for spatially developing direct numerical or large eddy simulations", *J. Comp. Phys.* Vol. 186, pp. 652-665.
- Li J., Zhao Z., Kazakov A., Dryer F., 2004, "An updated comprehensive kinetic model of hydrogen combustion", *Int. J. Chem. Kinetics*, Vol. 36, pp. 566-575.
- Pierce C., Moin P., 1998, "A dynamic model for subgrid scale variance and dissipation rate of a conserved scalar", *AIAA J.*, Vol. 36, pp. 1325-1327.
- Poinsot T., Veynante D., 2001, "Theoretical and Numerical Combustion", RT. Edwards.

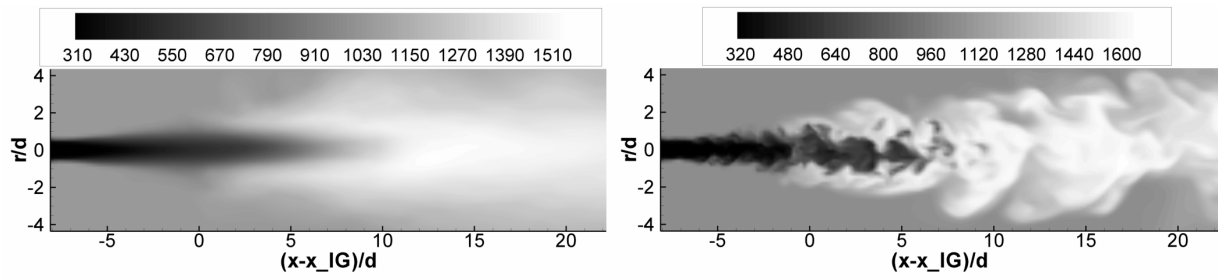


Figure 1: 2D cut of the instantaneous (right) and time averaged (left) temperature [K] fields.

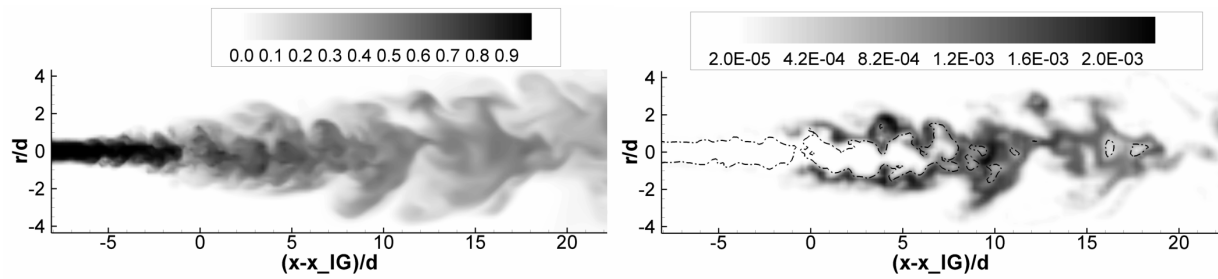


Figure 2: 2D cut of the instantaneous mixture fraction (left) and OH molar fraction (right) fields. The stoichiometric line ( $Z_{ST}=0.47$ ) is shown as a dashed line.

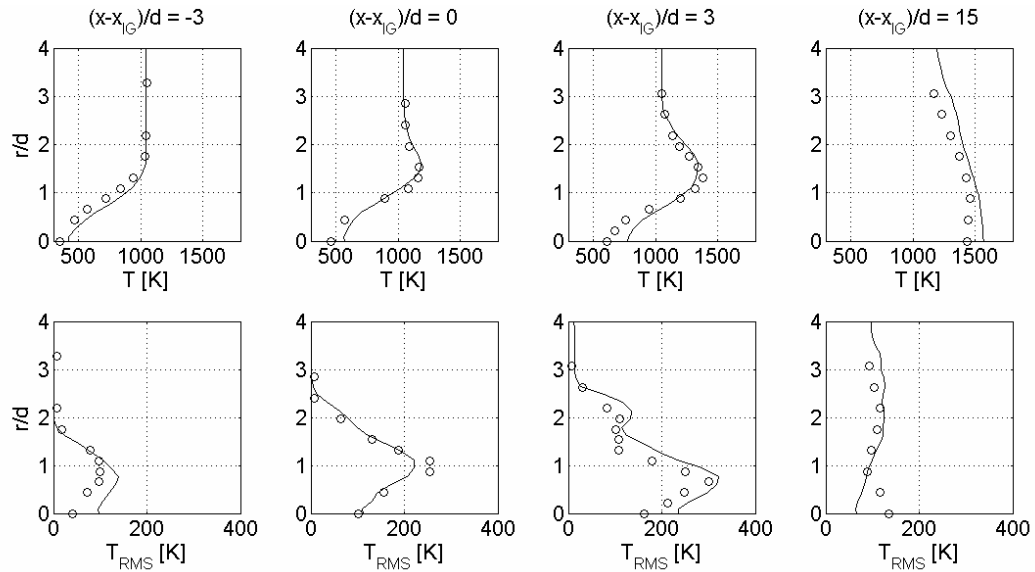


Figure 3: Mean temperature (top) and RMS of the temperature fluctuation (bottom) along different radial lines from LES (line) and experiments from Cabra and Dibble (2002) (symbols).

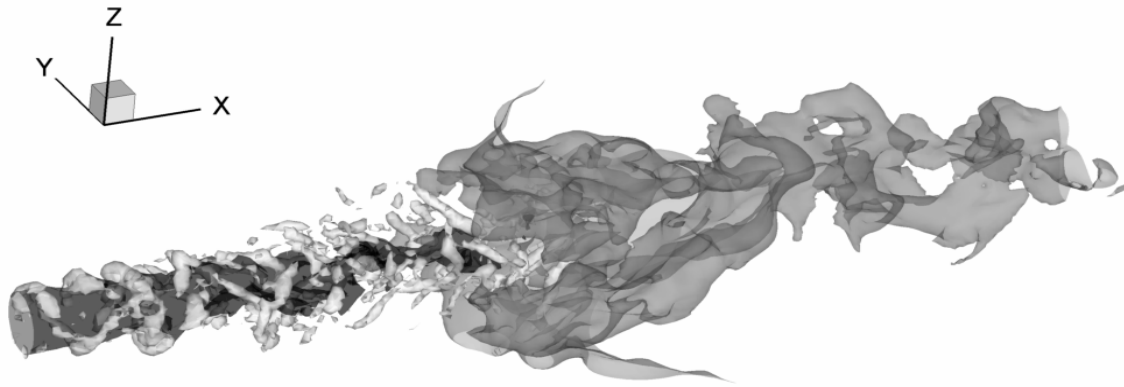


Figure 4: Snapshot of the temperature and vortex cores, iso-level:  $T=400\text{K}$  (black);  $T=1046\text{K}$  (dark gray) and  $\lambda_2=-10^{-3}$  (light gray).

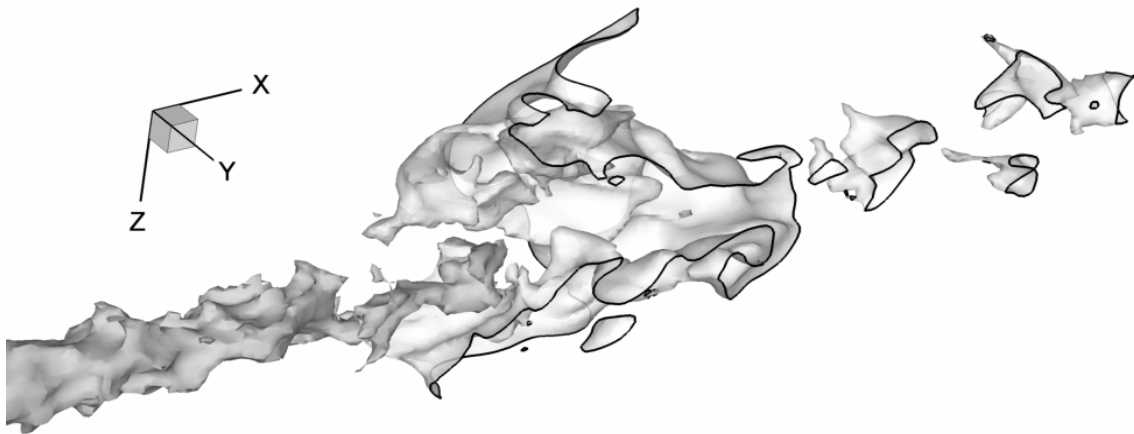


Figure 5: Zoom on the ignition region: snapshot of the temperature and vortex cores, iso-level:  $T=400\text{K}$  (dark gray);  $T=1046\text{K}$  (light gray). Only half of the second iso-level is represented.

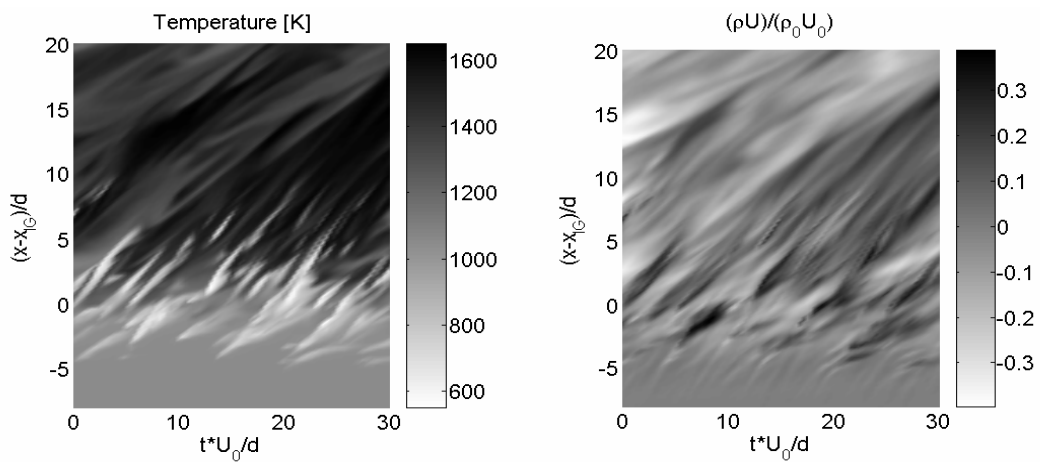


Figure 6: Temperature (left) and normalized axial momentum flux fluctuation (right) along an axial line  $r/d=1$  in a  $[x, t]$  diagram.